Original Research Article

The vacancy energy in metals: Cu, Ag, Ni, Pt, Au, Pd, Ir and Rh

ABSTRACT

The predictive calculations of vacancy formation energies in metals: Cu, Ag, Ni, Pt, Au, Pd, Ir and Rh are presented. The energy is given as a function of electron density. Density functional theory underestimates the vacancy formation energy when structural relaxation is included. The unrelaxed mono-vacancy formation, unrelaxed di-vacancy formation, unrelaxed di-vacancy binding and low index surface energies of the fcc transition metals Cu, Ag, Ni, Pt, Au, Pd, Ir and Rh has been calculated using embedded atom method. The values for the vacancy formation energies agree with the experimental value. We also calculate the elastic constants of the metals and the heat of solution for the binary alloys of the selected metals. The average surface energies calculated by including the crystal angle between planes (hkl) and (111) correspond to the experiment for Cu, Ag, Ni, Pt and Pd. The calculated mono-vacancy formation energies are in reasonable agreement with available experimental values for Cu, Ag, Au and Rh. The values are higher for Pt and Ir while smaller values were recorded for Ni and Pd. The unrelaxed di-vacancy binding energy calculated agrees with available experimental values in the case of Cu, Ni, Pt and Au.

Keywords: EAM; Energy calculations; Elastic constants; Heats of solutions.

INTRODUCTION

Interatomic potential models are numerous but issues on an excellent Interatomic potential model for computer simulation of metallic systems need to be addressed. Although there are so many developed models like effective medium theory (EMT), Glue model, modified embedded atom model (MEAM), model generalized pseudo-potential theory (MGPT) e.t.c, but the embedded-atommethod (EAM) is an extensivelyused technique (Daw et al., 1983) for the understanding of many-bodypotentialmodels.

Using the EAM, the energyneed to position an impurity atom in a lattice is taken as a function of the electron density. An atomicspecies at a particular site therefore has an unmatchedenergyfunction of the electron density (Puska et al., 1981). Through this belief, many authors have originatedseveralpotentialmodels. Finnis and Sinclair, 1984 developed a model which is mathematically analogous to the EAM. The functionalform of the energy of the EAM was deduce (Manninen, 1986) and (Jacobson et al., 1987) usingdensity-functionaltheory. Johnson (1988) developed a simple analytic model for fcc (face-centeredcubic) metalsusingnearestneighbordistance. This EAM function is sufficient only for nearest-neighbor interaction and the reliability has been investigated by calculating the vacancy energy in some selected fcc metals. Mei et al., 1990 procure a closet analytic form of embeddingfunction by chosen exponential chargedensity of interest, they obtainedpotential parameters for fcc metalsusing a third neighbormodel. Cai and Ye, 1996 assumed that the embeddingenergy of an atom should take the totalform of energypresented by Banerjea and Smith (1988).

There is existence of defect in a crystal lattice at temperatures above absolute zero and the presence of small amount of impurities may enhance vacancy formation in many metals and metal alloys (Laura, 2017). Thermodynamics has provided the possibility of estimating the defect concentrations

of metals at the equilibrium conditions even with good inter atomic potentials.For proper understanding of the defect trapping during solidification in pure metals, Zhang et al has performed molecular dynamics simulations for both aluminum and nickel and found that vacancies are dominant defects in the product crystals of both metals (Zhang et al, 2017).

It is now clear that everyone has the choice of potentials and embeddingenergy but the most excellent ones are those that can reproduce the significant parameters of the metals and alloys. In this paper, the employedpotentialutilized the totalform of the embeddingfunctionpresented by Mayer with two-bodypotentialof Rose et al., 1984. This potentialfunction was selectedfor it is very simpleform and is easy to be used in computersimulation. The potential parameters of this model are derived through fitting thelatticeconstant, elastic constants, cohesiveenergy, and vacancyformationenergyby optimization technique. Cheng et al., 2018 presented a new 3D metal-vacancy solid-solution NiAlP synthesized by combining selective alkali-etching and phosphorization strategies as a highly-active and earth-abundant pH bifunctional electrocatalyst for efficient water splitting.Vacancy coalescence of metallic oxide/alloy interface can result in the formation of low-density metal and eventually small sized voids (Richard et al, 2018).

The parameters have been used to calculate properties includingbulkmodulus, monovacancy formingenergy, divacancy formingenergy, divacancy bindingenergy, the surfaceenergy of the lowindexcrystal, and the elastic constants. Information concerning the groundstate properties of these metals is significant in mandate to know the kind of materials that can be formed from such metals. Zhang and Liu (2002) developed an embeddedatommethodpotential for Ni-Al alloys. Their declaration of the embeddedfunction was devised in analogy with the density function theory. Consistent empiricalembedded-atompotential that contains a longrangeforce for fcc metals and alloys has been developed to estimate the elastic constants and the heats of solution of some choice fcc metals (Iyad, 2009). The total energy of EAM is given as

$$E_{tot} = \sum_i F_i(\rho_i) + \frac{1}{2}\sum_{i,j} \phi_{ij}(r_{ij}) \qquad (1)$$

where

$$\rho_i = \sum_{j \neq i} f_{ij}(r_{ij}) \qquad (2)$$

The parameter $F_i(\rho_i)$ is the energy to embed an atom into the environment of the remaining atoms, ϕ_{ij} is an electrostatic two-body interaction between atoms i and j and $f_{ij}(r_{ij})$ is the local electron density, ρ is the host electron density. So far, from equation (1) the following functions $F(\rho)$, $\rho(r)$ and $\phi(r)$ are very important.

THEORY

In the Analytic Embedded Atom Method, the electron density is given by:

$$f(r) = f_e exp\left[-\beta\left(\frac{r}{r_o} - 1\right)\right] \qquad (3)$$

The embedding potential between atom i and atom j is given by:

$$\phi^{ij}(r) = \phi_e exp\left[-\gamma\left(\frac{r}{r_o} - 1\right)\right] \qquad (4)$$

The embedding function is determined using equation (5):

$$F(\rho) = -E_c\left[1 - \frac{\alpha}{\beta}ln\left(\frac{\rho}{\rho_o}\right)\right]\left[\frac{\rho}{\rho_o}\right]^{\frac{\alpha}{\beta}} - \Phi_e\left[\frac{\rho}{\rho_o}\right]^{\frac{\gamma}{\beta}} \qquad (5)$$

where $\rho_o = 12f_e$ and $\Phi_e = 6\phi_e$

To determine the two adjustable parameters f_e and ϕ_e for each metal, equation (6) was used.

$$f_e = \frac{SE_c}{\Omega_e} \quad \text{and} \quad \phi_e = \frac{E_c}{6} \qquad (6)$$

where S is an arbitrary scaling constant.

The parameters α, β and γ can easily be determined from equations $(7-9)$.

$$\alpha = 3\left(\frac{\Omega_e B}{E_c}\right)^{\frac{1}{2}} \tag{7}$$

$$\beta = \left(\frac{15 E_c \Omega_e G}{E_v(E_v+E_c)}\right)^{\frac{1}{2}} \tag{8}$$

$$\gamma = \left(\frac{15 \Omega_e G(E_c+E_v)}{E_c E_v}\right)^{\frac{1}{2}} \tag{9}$$

The elastic constants C_{11}, C_{12} and C_{44}, were calculated using equations (10), (11) and (12):

$$C_{11} = \frac{a_o^2}{2\Omega_e}\left[\left\{\varphi_e''(r) - \frac{1}{r_o}\varphi_e'(r)\right\} + 2F'(\rho_e)\left\{f_e''(r) - \frac{1}{r_o}f_e'(r)\right\}\right] \tag{10}$$

$$C_{12} = \frac{a_o^2}{4\Omega_e}\left[\left\{\varphi_e''(r) - \frac{1}{r_o}\varphi_e'(r)\right\} + 2F'(\rho_e)\left\{f_e''(r) - \frac{1}{r_o}f_e'(r)\right\}\right] + \frac{8a_o^2}{\Omega_e}\left(f_e'(r)\right)^2 F''(\rho_e) \tag{11}$$

$$C_{44} = \frac{a_o^2}{4\Omega_e}\left[\left\{\varphi_e''(r) - \frac{1}{r_o}\varphi_e'(r)\right\} + 2F'(\rho_e)\left\{f_e''(r) - \frac{1}{r_o}f_e'(r)\right\}\right] \tag{12}$$

The bulk modulus B and the shear modulus G, in equations $(7-9)$ is determined from equations (13) and (14) respectively.

$$B = \frac{1}{3}(C_{11} + 2C_{12}) \tag{13}$$

$$G = \frac{1}{5}(C_{11} - C_{12} + 3C_{44}) \tag{14}$$

Energy Calculations:

Vacancy migration which most oftenleads to vacancyforming is the controllingmovement behind atomiccarriage in most elemental crystals, and is of underlyingconsequence in proceduresimilarto solidphase transformations and faultmigration. Vacancy formationimplies the removal of an atom from the interior of a crystal. At thermal equilibrium as the vibration increases with increasing energy, the orientation of the atoms within the crystal changes. At lower thermal energy, the atoms are relaxed to a state of quasi thermal equilibrium.

The unrelaxed mono-vacancy forming energy is calculated using equations (15) and (16)

$$E_{1v}^{uf} = -12F(\rho_e) + 12F\left(\frac{11}{12}\rho_e\right) - 6\phi_e \tag{15}$$

$$E_{1v}^{uf} = -12E_n + 12E_{n-1} \tag{16}$$

where E_n is the total energy of the system having no vacancy.

The unrelaxed di-vacancy formation energy can be computed using equation (17)

$$E_{2v}^{uF} = -18E_n + 14E_{n-1} + 4E_{n-2} \tag{17}$$

The unrelaxed di-vacancy binding energy is calculated using:

$$E_{2v}^{uB} = 2E_{1v}^{uf} - E_{2v}^{uf} = -6E_n + 10E_{n-1} - 4E_{n-2} \tag{18}$$

The low index surface energy can be computed with equations (19) to (20):

The number of bonds broken on (111) surface $= (3\ bonds/atom)\times(1 atom/unit\ cell)$

Therefore number of bonds broken on (111) surface $= 3/(\frac{\sqrt{3}}{4}a_o^2)$

$$E_{surf} = E_{12-3} = E_9 \; ; \; E_{bulk} = E_n = E_{12}$$

$$\Gamma_{111}^{U} = N_s/A(E_9 - E_{12})$$

where N_s is the number of atom on the surface.

$$\Gamma_{111}^{U} = \frac{4}{a_o^2\sqrt{3}}(E_9 - E_{12}) \tag{19}$$

Similarly for Γ_{100}^{U} and Γ_{110}^{U} we have

$$\Gamma_{100}^{U} = \frac{2}{a_o^2}(E_8 - E_{12}) \tag{20}$$

$$\Gamma_{110}^{U} = \frac{\sqrt{2}}{a_o^2}(E_7 + E_{11} - 2E_{12}) \tag{21}$$

The crystal angle between planes (*hkl*) and (111) is calculated using

$$\cos\theta_{(hlk)} = \frac{(h+l+k)}{\sqrt{3(h^2+k^2+l^2)}} \tag{22}$$

Alloy potentials and heats of solutions

In computing the alloys pair potentials, the mixing rule in equation (23) was used

$$\phi^{ab}(r) = \frac{1}{2}\left[\frac{f^a(r)}{f^b(r)}\phi^{aa}(r) + \frac{f^b(r)}{f^a(r)}\phi^{bb}(r)\right] \tag{23}$$

and the heats of solution for b- typeatomas an impurity and a -typeatom as the host is computed by the summation of equations (24 – 29).

Remove host : $\qquad H_1 = -F^a(\rho_e^a) - \phi^{aa}(r_e^a) \tag{24}$

Add impurity : $\qquad H_2 = +F^a(\rho_e^a) + \Sigma\,\phi^{ab}(r_e^a) \tag{25}$

Adjust neighbours: $\qquad H_3 = -F^a(\rho_e^a) + F^a(X) \tag{26}$

where $\qquad X = \rho_e^a + \Delta\rho \tag{27}$

and $\qquad \rho = -f^a(r_e^a) + f^b(r_e^a) \tag{28}$

Adjust cohesive energy: $\qquad H_4 = -E_c^a + E_c^b \tag{29}$

Hence, $\qquad H = H_1 + H_2 + H_3 + H_4 \tag{31}$

It is essential to include lattice relaxations in many calculations involving energies [1]. The relaxation energy is given as:

$$H_r = -\left[1.167\left(\frac{\Omega_{ea}}{\Omega_{eb}} - 1\right)\right]^2 \tag{32}$$

Here, ρ_e^a is the equilibrium electron density of a–type atoms,

$_{ea}$ is the atomic volume of a - type atoms and

$_{eb}$ is the atomic volume of b - type atoms.

Table 1.0: Experimental data used in fitting procedure are: equilibrium lattice constants (a_o), cohesive energy E_c, vacancy formation energy E_{1v}^{uf} and the elastic constants: (C_{11}, C_{12}, C_{44} in $ergcm^{-3}$(column 5 - 7)) and $eV/Å^3$(column 8 – 10). The elastic constants: C_{11}, C_{12}, C_{44} in the last three column was converted from $ergcm^{-3}$ to $eV/Å^3$.

S/N	Atom	a_o (Å)	E_c (eV)	E_{1v}^{uf} (eV)	C_{11}	C_{12}	C_{44}	C_{11}	C_{12}	C_{44}
1	Cu	3.615^a	3.54^c	1.30^h	1.670^a	1.240^a	0.760^a	1.04	0.77	0.47
2	Ag	4.090^a	2.85^c	1.10^h	1.240^b	0.934^b	0.461^b	0.77	0.58	0.29
3	Ni	3.520^a	4.45^c	1.70^i	2.465^b	1.473^b	1.247^b	1.54	0.92	0.78
4	Pt	3.920^a	5.77^c	1.60^i	3.470^b	2.510^b	0.765^b	2.17	1.57	0.48
5	Au	4.080^c	3.93^c	0.90^h	1.860^b	1.570^b	0.420^b	1.16	0.98	0.26
6	Pd	3.890^c	3.91^c	1.54^i	2.341^b	1.760^b	0.712^b	1.46	1.10	0.44
7	Ir	3.840^c	6.94^c	1.80^d	5.990^b	2.560^b	2.690^b	3.74	1.60	1.68
8	Rh	3.800^c	5.75^c	1.71^g	4.220^b	1.920^b	1.940^b	2.63	1.20	1.21

Refs: [a](Folies *et al.*, 1986) ; [b](Simmons and Wang, 1971); [c](Kittel, 1996); [d](Landolt-Bornstein, 1991) ; [e](Ziesche and Perdew, 1994); [f](Sisoda and Verma, 1989) ; [g](De Boer *et al.*, 1988); [h](Ballufi, 1978); [i](Johnson, 1989); [j](Ghorai, 1991).

RESULTS AND DISCUSSION

Table 2.0 : Calculated input parameters $_e, B, G$ and model parameters $f_e, \varphi_e, \alpha, \beta$ and γ

S/N	Metal	(Å^3)	$B(\text{eV/Å}^3)$	$G(\text{eV/Å}^3)$	$\bar{f_e}$ (eV)	$\bar{\varphi_e}$ (eV)	α	β	γ
1	Cu	11.81	0.86	0.34	0.30	0.59	5.09	5.81	7.94
2	Ag	17.10	0.65	0.21	0.17	0.47	5.91	5.96	8.26
3	Ni	10.90	1.13	0.59	0.41	0.74	4.98	6.41	8.86
4	Pt	15.06	1.77	0.41	0.38	0.96	6.44	6.70	8.56
5	Au	16.98	1.04	0.19	0.23	0.66	6.36	6.67	8.20
6	Pd	14.72	1.22	0.34	0.27	0.65	6.43	5.90	8.23
7	Ir	14.16	2.31	1.44	0.49	1.16	6.51	10.98	14.09
8	Rh	13.72	1.68	1.01	0.42	0.96	6.00	12.05	14.54

9

Table 3.0: Calculated formation $E_{2v}^{uF}(eV)$, binding $E_{2v}^{uB}(eV)$, and low index surface $\Gamma_{(hlk)}^{U}(\frac{ergs}{cm^2})$ energies. The present work is listed first (values with asterisk include $cos\theta_{(hlk)}$). The experimental values are listed second, and the results of other authors are listed last.

S/N	Atom	$E_{2v}^{uF}(eV)$	$E_{2v}^{uB}(eV)$	$E_{2v}^{uF}(eV)$ Γ	$\gamma_{11}\times10_3$	$\gamma_{00}\times10_3$	$\gamma_{10}\times10_3$	$\gamma_{ve}\times10_3$
1	Cu	2.41	0.19 0.13 ± 0.04^{l}, 0.3^{m} 0.27^{a}	1.31 1.3^{h} 1.28^{a}	1.02, 1.02*	1.23, 2.14*	1.34, 1.64*	1.20, 1.60 1.77^{q} 1.28^{a}, 1.57^{q}
2	Ag	2.13	0.15 0.38^{n} 0.22^{a}	1.14 1.10^{h}	0.70, 0.70*	0.86, 1.49*	0.94, 1.15*	0.83, 1.11 1.32^{q} 0.70^{a}, 1.19^{q}
3	Ni	3.15 $2.92-3.10^{a*}$	0.27 0.33^{p}, 0.28^{l*} 0.44^{a}	1.71 1.80^{d}	1.32, 1.32*	1.56, 2.71*	1.69, 2.06*	1.52, 2.03 2.24^{q}
4	Pt	3.29	0.19 $0.1-0.2^{h}$ 0.45^{a}	1.74 1.60^{i}	1.24, 1.24*	1.56, 2.70*	1.72, 2.10*	1.51, 2.02 2.50^{**} 1.61^{a}, 1.99^{q}
5	Au	1.93	0.09 0.1 ± 0.03^{r}, 0.3^{t} 0.22^{a}	1.01 0.90^{h}	0.70, 0.70*	0.89, 1.54*	0.99, 1.21*	0.88, 1.15 1.54^{q} 0.90^{a}, 1.03^{q}
6	Pd	3.10	0.20 0.34^{a}	1.65 1.70^{i}	1.15, 1.15*	1.41, 2.45*	1.54, 1.89*	1.37, 1.82 2.00^{**} 1.36^{a}, 1.57^{q}
7	Ir	3.64	0.32	1.98 1.80^{d}	1.25, 1.25*	1.47, 2.54*	1.58, 1.93*	1.43, 1.91 3.00^{**} 2.84^{a}
8	Rh	3.14	0.28	1.71 1.71^{g}	0.78, 0.78*	0.91, 1.58*	0.98, 1.20*	1.28, 1.72 2.60^{**}

Refs: ^{a}(Folies et al., 1986); ^{d}(Landolt-Bornstein, 1991) ; ^{e}(Ziesche and Perdew, 1994); ^{g}(Ledbetter and Kim, 2001) ; ^{h}(Ballufi, 1978); ^{i}(Johnson, 1989) ; ^{j}(Ghorai, 1991) ; ^{l}(Seeger et al., 1963); ^{l*}(Seeger and Schumacher, 1967) ; ^{m}(Fluss et al., 1980); ^{n}(Kraftmakher and Strelkov, 1970) ; ^{p}(Mehrer et al., 1965) ; ^{q}(Baskes, 1992); ^{r}(Bauerle and Koehler, 1957); ^{t}(Meshii et al., 1962) ; ^{u}(Ehrhart et al., 1991); ^{a*}(Nanao et al., 1977).

The calculated surface energies for the low index crystal faces are compared to the experimental polycrystalline average values (eV/cm^2). The values indicated by an asterisk was extrapolated from the melt temperature to 0K (Baskes, 1992).

Table 4.0: Calculated and experimental properties of pure metals. The first lines present the experimental values of elastic constants in $eV/Å^3$ (column 3 – 5) and Bulk modulus in $eV/Å^3$ (column 6). The second lines present the predicted values using common cut-off radius $1.11r_e \geq r_c \leq 1.25r_e$.

S/N	Metal	c_{11}	c_{12}	c_{44}	B
1	Cu	1.04[a]	0.77[a]	0.47[a]	0.86[g]
		1.03	0.57	0.53	0.72
2	Ag	0.77[b]	0.58[b]	0.29[b]	0.60[g]
		0.77	0.43	0.40	0.54
3	Ni	1.54[b]	0.92[b]	0.78[b]	1.16[g]
		1.53	0.84	0.79	1.07
4	Pt	2.17[b]	1.57[b]	0.48[b]	1.77[g]
		1.87	1.02	0.96	1.30
5	Au	1.16[b]	0.98[b]	0.26[b]	1.08[g]
		1.18	0.65	0.61	0.83
6	Pd	1.46[b]	1.10[b]	0.44[b]	1.21[g]
		1.66	0.97	0.88	1.20
7	Ir	3.74[b]	1.60[b]	1.68[b]	2.22[b]
		3.72	1.97	1.90	2.55
8	Rh	2.63[b]	1.20[b]	1.21[b]	1.68[*]
		2.53	1.33	1.28	1.78

Refs: [a](Folies *et al.*, 1986); [b](Simmons and Wang, 1971) ; [d](Landolt-Bornstein, 1991) ; [f](Sisoda and Verma, 1989) ; [g](De Boer *et al.*, 1988) ; [*]Computed using equation (8)

Table 5.0: Heats of solution for the likelybinaryalloys of the chosen fcc metals. The results of the unrelaxed calculations are listed first, the values with relaxation second, the experimentalvalues (Ref. v and w) where valid, and the adaptedvalues from other author (Ref. q and y) are listed last.

Impurity	Host							
	Cu	Ag	Ni	Pt	Au	Pd	Ir	Rh
Cu		0.40 0.27 0.25^v	0.11 0.10 0.11^v	-0.19 -0.26 -0.30^v	0.05 -0.08 -0.13^v	0.10 0.05 -0.39^v	-0.29 -0.33 -0.64^q	-0.17 -0.20 -0.72^q
Ag	0.79 0.52 0.39^v		1.88 1.44	0.65 0.63	-0.06 -0.06 -0.16^v	0.32 0.28 -0.11^v	1.37 1.31 0.78^q	1.12 1.02
Ni	0.08 0.07 0.03^v	0.75 0.57		-0.12 -0.23 -0.33^v	0.33 0.19 0.22^v	0.22 0.21 -0.09^v	-0.34 -0.41 -0.25^q	-0.14 -0.20 -0.35^q
Pt	-0.30 -0.40 -0.53^v	0.66 0.64	-0.23 -0.43 -0.28^v		0.46 0.46	-0.03 -0.03	0.17 0.16	0.02 0.01
Au	-0.01 -0.27 -0.19^v	-0.03 -0.03 -0.19^v	0.84 0.42 0.28^v	0.58 0.56		-0.03 -0.06 -0.20^v	1.47 1.42 0.57^q	0.91 0.84 0.37^q
Pd	0.15 0.06 -0.44^v	0.30 0.28 -0.29^v	0.69 0.53 0.06^v	-0.01 -0.01	0.01 -0.01 -0.36^v		0.43 0.43	0.26 0.25
Ir	-0.94 -0.99 -0.73^q	0.66 0.62 0.55^q	-1.29 -1.41 -0.68^q	0.07 0.06	0.51 0.47 0.38^q	-0.06 -0.06 -0.28^q	-	0.004 0.006
Rh	-0.44 -0.48 -0.74^q	0.52 0.47 0.35^q	-0.47 -0.56 -0.55^q	-0.01 -0.00	0.32 0.27 0.24^x	0.03 0.03 -0.35^q	-0.04 -0.04	-

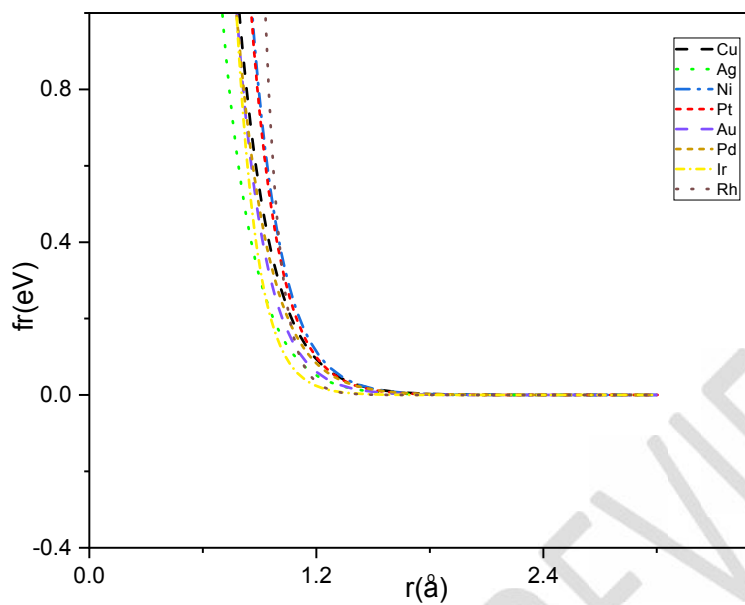Refs: [q](Baskes, 1992); [w](Miedema*et al*., 1980) ; [v](Hultgren*et al*., 1973) ; [y](Iyad, 2009)

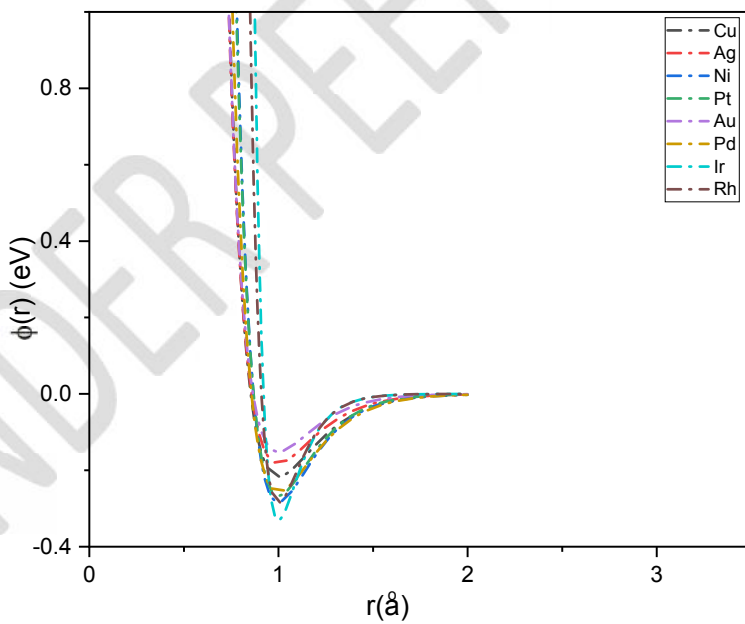Fig.1: Characteristics of the electron density function for the selected metals.

Fig. 2: Characteristics of the pair-potential function for the selected metals.
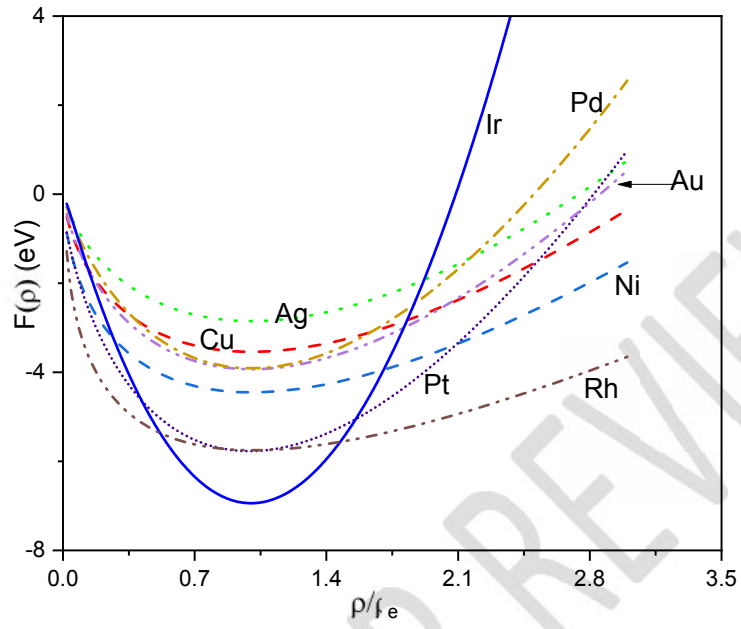
Fig. 3: Characteristics of the embedding energy function for the selected metals.
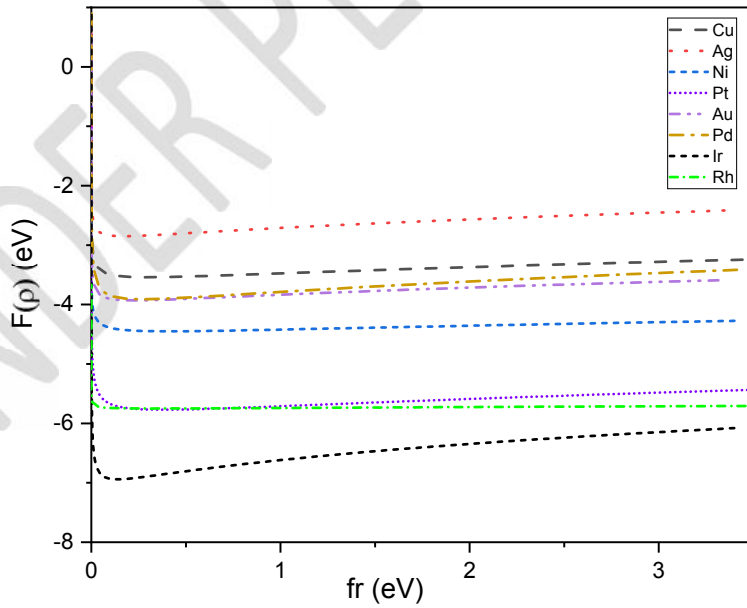

Fig. 4: Characteristics of the embedding energy function
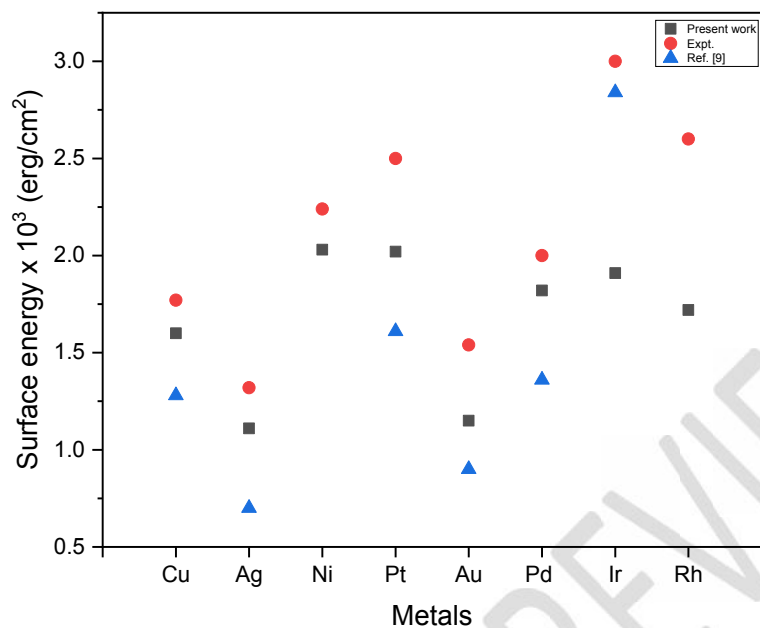with electron density for the selected metals.

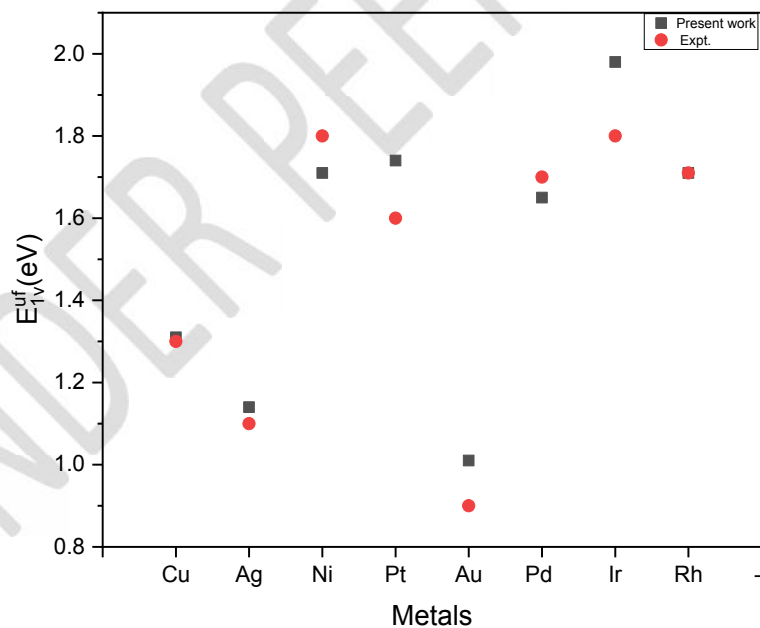Fig. 5: Plot of unrelaxed surface energies for the selected metals.

Fig. 6: Plot of unrelaxed mono-vacancy formation energies for the selected metals.
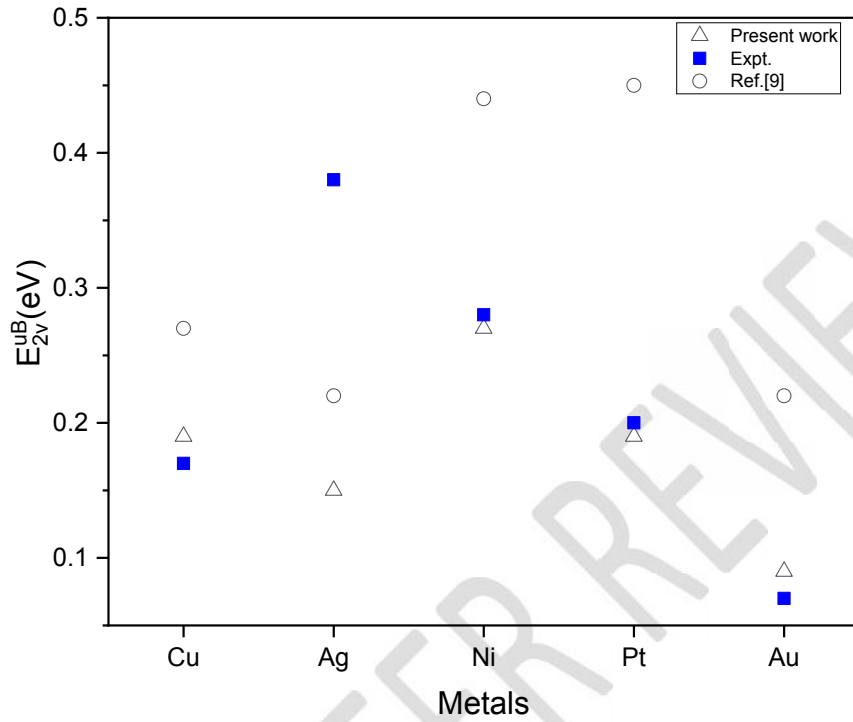
Fig. 7: Plot of unrelaxed di-vacancy binding energies for some of the selected metals.

In Fig.1, the electron density $f(r)$ displays the common characteristics for the selected metals.

Fig. 2 shows the least (minimum) free energy curves for the electron which gives the equilibrium interatomic distance. The width of the curves increases as the values of r increases, therefore the position of the principal minimum is displaced to larger values of r. The pair-potential tends to group Cu, Ag, Ni, Pt, Au and Pd, also Ir and Rh.

In Fig. 3, there are systematic trends in the embedding energies. The curvature of the embedding function accounts for the "many-body" aspect of the model with the least embedding energy occurring for Ir.

Fig. 4. shows that the embedding function goes through the appropriate range of electron densities and the characteristics curves tends to group: Cu, Pd with Au and also Pt with Rh.

Fig. 5. presents the unrelaxed surface energies for the selected metals while Fig. 6 and Fig. 7 give the plots of the unrelaxed mono-vacancy formation and di-vacancy binding energies respectively.

The properties calculated in this work will help in finding new metals/compounds for substitution in alloying processes. The ground state properties such as, surface energies, vacancy formation energies and heats of solutions has been calculated. The sensitivity of the heats of solutions on the embedding function and the potential produces good results in comparison with the available experimental values.

Finding new metals/compounds for substitution in alloying processes is an issue that needs to be addressed by the material scientist especially in this state of scarcity in the case of palladium. The calculated mono-vacancy formation energies are in reasonable agreement with available experimental values for Cu, Ag, Au and Rh as shown in Fig. 6. The values are higher for Pt and Ir while smaller values were recorded for Ni and Pd. The unrelaxed di-vacancy binding energy calculated agree with available experimental values closer than the results of Folies *et al.*, 1986 in the case of Cu, Ni, Pt and Au (See Fig. 7).

The unrelaxed surface energy for the three fcc low-index planes was estimated by dividing the total energy increase in separating bulk material on a crystallographic plane by the total new surface area created. In all the cases, the trends $E_{(111)} < E_{(100)} < E_{(110)}$ was observed and also by including crystal angle between planes, we have $E_{(111)} < E_{(110)} < E_{(100)}$. The lowest surface energy corresponds to the closed-packed (111) plane as observed in Table 3.0. Therefore closed packed surfaces looks most stable for fcc metals. The calculated average surface energies are closer to the experimental values than those obtained by the MEAM (Baskes, 1992).

The average surface energies predicted low average values compared to the available experimental values but when the crystal angle was included, moderate average values were obtained and they are in good agreement with the available experimental values for Cu, Ag, Ni, Pt and Pd. The results for Cu, Pt, Au and Pd are closer to the experimental values than that of Ref. (Folies *et al*., 1986) (See Fig. 5) and (Baskes, 1992) (See Table 3.0).

SUMMARY

The calculated ground state properties for the pure metals include surface energies, mono-vacancy formation energies, di-vacancy formation energies, di-vacancy binding energies, elastic constants and their heats of solutions. The agreement between the experiment and the calculated values is quite good for the metals and their alloys. From the heats of solutions calculated (Table 5.0), the

positive heats of solution recorded are higher than the negative heats of solutions. The most negative heats of solution occur for the relaxation values and most positive occurs for the unrelaxed values. The pair potential function of the alloy mixing '$\varphi(r)^{ab}$' between two different atoms *a* and *b* gives reasonable values of heats of solutions in the case of Cu, Ag, Au, Ni and Pt.

CONCLUSION

The EAM model was used to compute some ground state properties of the selected fcc transition metals and their binary alloys. The di-vacancy binding energies calculated also agree with the available experimental values. The surface energies predicted by the model was low in comparison to experiments but when the crystal angle was included, the model predicted low index surface energies that agree reasonably with the experiment in better comparison with the values from Ref. (Foiles *et al*., 1986) and (Baskes, 1992). The model is well-suited for studies of defects energies in metals and their alloys. The surface energies calculated by including the crystal angle between

planes corresponds to the experiment for Cu, Ag, Ni, Pt and Pd. For surface energy minimization, it is good that the (111) texture should be favoured in an fcc film. The embedding function $F(\rho)$ with the angle between planes (*hkl*) and (111) can be used to estimate the relative values of surface energy for surfaces in different orientations.

REFERENCES

Ballufi RW. *J Nucl. Matter*. 1978, 69 & 70:240.

Banerjea A and Smith J.R. *Phys. Rev. B*. 1988, 37, 6632.

Baskes M I. *Phys. RevB*. 1992; 46:2727.

Bauerle JE and Koehler JS. 1957. 107:1493.

Cai J. and Ye YY.: *Phys. Rev. B*.1996, 54, 8398.

Cheng Weiren, Zhang Hui, Zhao Xu, Su Hui, Tang Funmin, Tian Jie and Lui Quinghua *Journals of Materials Chemistry A*. 2018, 20: 1- 19.

Daw MS, Bisson CL and Wilson WD. *Solid commun*. 1983;46.

De Boer FR, Boom R, Mattens WCM, Miedema AR and Niessen AK. *Cohesion in Metals*, Vol. 1. Amsterdam: North Holland. 1988.

Ehrhart P, Jung P, Schultz H and Ullmaier H. Atomic Defects in Metals. *Springer Verlag*. Edited by Ullmaier .H. *Landolt-Börnstein*. New Series. Group III/25, Berlin; 1991.

Finnis MW and Sinclair JE. *Philos. Mag. A*.1984, 50, 45.

Fluss MJ, Smedskjaer LC, Siegel RW, Longini DG and Chason MK. *J. Phys*. F. 1980,10:1763.

Foiles SM, Baskes MI and Daw MS. *Phys.Rev. B*. 1986, 33:7983.

Ghorai A. *Physica Status SolidiB*. 1991, 167:551.

Hultgren R, Desai PD, Hawkins DT, Gleiser M and Kelley KK. Selected Values of the Thermodynamic Properties of Binary Alloys (American Society for Metals, Metals Park,OH); 1973.

Iyad AH, Young P. *J. Mater. Sci. Technol*.2009, 25:6.

Jacobson KW, NÁrskov JK and Puska J. *Phys. Rev. B*.1987, 35, 7423.

Johnson RA. *Phys. Rev.B*. 1989, 39, 17:12554 – 12559.

Johnson RA. *Phys. Rev. B*.1988, 37, 3924.

Kittel C. Introduction to Solid State Physics. 7th Edition. John Willey & Sons. Inc., New York, Chicester, Brisbarne, Toronto, Singapore. 1996, 28 – 98.

Kraftmakher YA and Strelkov PG. In Vacancies and Interstitials in Metals, edited by Seeger A., Schumacher D, Schilling W and Diehl J. (North-Holland), Amsterdam. 1970, 59.

Landolt-Bornstein. New Series, Vols. III-11 and III-18 Berlin: *Springer-Verlag*. 1991.

Laura Bukonte. Modelling of defect formation and evolutionin metals and silicon. Division of Materials Physics, University of Helsinki-Helsinki, Finland. 2017, 1- 66. ISBN 978-951-51-2768-6.

Ledbetter H and Kim S. Monocrystal Elastic Constants and Derived Properties of The Cubic and The Hexagonal Elements, in: Handbook of Elastic Properties of Solids, Liquids and Gases, Academic Press. 2001, Vol. 2.

Manninen M. *Phys. Rev. B*.1986, 34, 8486.

Mehrer H, Kbonmuller H and Seeger H. *Phys. Stat. Sol*. 1965, 10:725.

Mei J, Devenport JW and Fernando G.W. *Phys. Rev. B*.1990, 43, 4653.

Meshii M, Mori T and Kauffman JW. *Phys. Rev*. 1962, 185:1239.

Miedema AR, de`Chatel PF, de Boer FR . *Physica B*.1980, 100:1.

Nanao S, Kuribayashi K, Tanigawa S and Doyama M. *J. Phys. F: Met. Phys*. 1977, 7:1403.

Puska J, Nieminen RM and Manninen M. *Phys. Rev. B*.1981, 24, 3037.

Richard P. Oleksak, Monica Kapoor, Daniel. E. Perea, Gordon R. Holcomband Ömer N. Doğan. *npj Materials Degradation*. 2018, 25:1-8.

Rose JH, Smith JR, Guinea F and Ferrante J. *Phys. Rev. B*.1984, 29, 2963.

Seeger A, Gerold V, Chik KP and Ruhle M. *Phys. Letters.* Netherlands. 1963, 6:107.

Seeger A and Schumacher D. *Mater. Sci. Eng*. 1967, 2:31

Simmons G and Wang H. Single Crystal Elastic Constants and Calculated Aggregate Properties: A Handbook (MIT Press, Cambridge); 1971.

Sisoda P and Verma MP. Shear Moduli of Polycrystalline Cubic Elements. *J. Phys. Chem. Solids*. 1989, 50:223 – 224.

Zhang, H. Y. Lu. F, Yang. Y and Sun .D.Y. *Scientific reports*. 2017, 7:10241, 1-8.

Zhang RF and Liu BX. Proposed model for calculating the standard formation enthalpy of binary transition-metal systems. *Appl. Phys. Lett* 2002, 81, 1219–1221.

Ziesche P, Perdew JP and Fiolhais C. Spherical Voids in the Stabilized Jellium Model: Rigouruos Theorems and Pad; Representation of the Void-Formation Energy. *Phy. Rev. B*. 1994, 49:7916.